

Fabrication, Characterization and Deformation Behavior of a New Acrylate Copolymer-based Nonwoven Structure

David N Githinji*, John T Githaiga, David R Tuigong, Diana S Madara
Bernard Kipsang and Silas Khasindu

Department of manufacturing, Industrial & Textile Engineering, Moi University
P.O. Box 3900-30100, Eldoret, Kenya

Abstract

A method of fabricating nonwoven structure from dry-laid cotton fibers and atomized acrylate copolymer is presented. The method based on a consolidation pressure of about 2kPa and room temperature curing, is used to produce structures with fiber mass to binder volume ratio (FBR) of 0.7, 0.5, 1, 1.5, 2 and 3. Structurally stable structures are produced and characterized in terms of their bursting strength, areal density, water absorption, and monotonic deformation behavior. At constant FBR, the bursting strength and areal density of the structures increases with the fiber mass. The structures' water absorption capacity reduces with the increase in the volume of binder applied. At FBR of 1 and area density of 295 grams per square meter, the structure's load-strain curve is characterized by a linear and non-linear behavior corresponding to elastic and inelastic strain, respectively. At peak loads, the structure's deformation is relatively uniform but becomes localized as the failure point is approached. A good correspondence is established between the strain assessment based on uniaxial tensile test and on image correlation using Particle Image Velocimetry (PIV) method. The average vector magnitude derived from PIV measurement, correlate well with the engineering strain and can thus be used for strain estimation.

Keywords: Nonwoven, Dry-laid, Deformation, Particle Image Velocimetry, acrylate copolymer

Introduction

Nonwoven structures consist of web of directional or random orientated fibers bonded together. The web made up of natural, synthetic or man-made fibers can either be wet-laid or dry-laid (Batra & Pourdeyhimi, 2012). Wet-laying entails suspending fibers in water, draining and drying resulting in randomly oriented web of fibers while dry-laying involves mechanically orientating fibers into a web through combing processes. To obtain structurally stable structure, the web is bound through techniques such as felting, adhesive bonding, thermal bonding, needle punching, hydroentangling or spinlaying (Russell, 2007).

Natural fibers such as cotton are used in medical and hygiene nonwoven products because of their high absorption capacity, comfort, softness, chemical resistance and biodegradability. To produce lightweight structures, adhesive bonding is often used to bind the fibers. For stiff and compacted products, adhesive (binder) is mainly applied through saturation method but for open and bulky products, spraying method is used which ensures controlled application of binder, uniform binder application and a soft handle (Russell, 2007;

Adanur, 1995). Chemically, the binders are synthetic lattices such as acrylic latex, styrene-butadiene latex and vinyl acetate latex. The lattices contain surfactant to disperse the polymer particles and to aid in fiber wetting. Drying of binder after application ensures agglomeration of polymer particles which subsequently crosslink with itself to form an insoluble network around and through the fiber contacts. Formation of covalent bonds between cellulose molecules and polymer particle may also take place depending on the chemical nature of the polymer and the curing temperature.

Deformation of nonwoven structures under various loading conditions has been studied severally (Desai & Balasubramanian, 1994; Das & Raghav, 2009; Gautier, et al., 2007) focusing mainly on their mechanical properties. There is little published information on the areal deformation behavior of nonwoven structures under uniaxial or biaxial stress. Image processing technique has been applied in the areal measurement of fiber orientation in nonwoven (Wang, et al., 2014) and in mapping strain qualitatively in nonwoven structures under uniaxial load (Ridruejoa, et al., 2011). The use of image correlation technique to quantitatively characterize deformation in nonwoven structure has not been explored extensively in the literature. The current work aims at contributing in this area through use of Particle Image Velocimetry (PIV) plug-in installed in the ImageJ software (Abramoff, et al., 2004). PIV is a displacement measuring technique of small particles embedded in a region of a fluid. The theory, working principle and applications of PIV is expounded in several studies (Westerweel, 1993; Westerweel, 2000; Westerweel, 1997; Willert, 1996; Willert & Gharib, 1991). The method works by recording at different times, the light reflection from tracer particles in a flowing medium, thus allowing evaluation of their displacement. A typical PIV setup consists of a digital camera, light source and image analysis software. For accurate PIV assessment, the camera setting and lighting are maintained constant during the measurement. The particle movement from one point to another is quantified in terms of vector magnitude. In the current study, the deformation at a constant rate in a novel nonwoven structure was analyzed using PIV which allowed both qualitative and quantitative assessment of damage evolution.

Materials and Methods

Materials

Fabrication of nonwoven structure was based on cotton fibers characterized by the following average values: 26mm fiber length, 25g/Text fiber strength, 6.3% fiber elongation, 79.3% uniformity index, 13.2% short fiber content, 2.6% trash content, 4.1 micronaire value, 0.85 degree of maturity and high degree of white. The textile binder used was a colloidal and surfactant stabilized copolymer of vinyl acetate and acrylic esters monomers having a solid content of 33%, a pH of 6-7.5, a viscosity of 20-200cPs and a specific gravity of 1.04. The binder was diluted with distilled water at a ratio of 1:1 before application.

Methods

Fabrication of nonwoven structure

Cotton fibers were passed through a trash analyzer machine for cleaning and opening up into nearly individual fiber state. Samples weighing 5g, 10g, and 15g were taken from the opened fibers. Each sample was spread uniformly on a plastic plate previously coated with a thin layer of glycerine. A controlled amount of textile binder was sprayed uniformly on the laid fibers at a fiber mass to binder volume ratio of 0.7, 0.5, 1, 1.5, 2 and 3. Each assembly was then cold pressed at a uniform pressure of about 2kPa for 10 minutes followed by room temperature drying and curing for 12 hours.

Characterisation of nonwoven structure

The areal density in terms of grams per square meter (GSM) of the fabricated structures was determined in accordance with KS 08-1038:1990 – Part 1 of the Kenyan standards. Circular samples of about 100 cm² were cut and weighed on a digital balance. An average GSM value was then computed for each nonwoven structure fabricated.

The bursting strength of the structures was determined in accordance with KS ISO 13938 – Part 2 of the Kenyan standards. Uster bursting strength tester was used where a circular specimen was pneumatically clamped and pressure applied on it via a diaphragm. The maximum pressure supported by the structure before failure was recorded as the bursting strength.

The intrinsic water absorbency of the fabricated structures was determined by computing the weight difference between an oven dry structure and a wet structure which had been immersed in distilled water for 60 seconds and allowed to drip for 60 seconds. Intrinsic absorbency was expressed as the weight of the imbibed water per unit mass of the structure.

The microscopic examination of the nonwoven structure was based on a digital optical microscope (Zeiss Axiotech). Samples were mounted on the microscopic and different regions examined to allow a general assessment of the fiber bonding and distribution.

Tensile tests were conducted on a Universal Tensile Tester machine (rycobel TH2730) in accordance with KS 08-1038:1990 – Part 1 of the Kenyan standard. The tests were performed in displacement controlled mode at a constant rate of 200mm/min crosshead speed using a gauge length of 70mm and a specimen width of 5mm. A digital camera (Nikon D3100 14.2 MP with 18-55mm VR Lens) was used to capture sequential images of the structure during the tensile loading. For every 5mm extension in the structure, an image was captured and this was repeated until the structure failed. ImageJ software installed with a PIV plug-in was used to qualitatively analyze the uniformity of surface deformation using vector magnitude maps. This was achieved by correlating a zero strained image with an image captured at a higher strain level. The strain built-up after each extension interval was quantified by averaging the vector magnitudes of all elements displacement in the camera field of view.

Results and Discussion

Table 1 summarizes the densities, bursting strengths and intrinsic absorbencies of the nonwoven structures fabricated at various ratios of fiber mass to binder volume (FBR). At constant FBR, the density and bursting strength of the structures increased with increasing fiber mass. In these structures, the fibers thus provide the loading bearing capacity and so the strength increases with the fiber content. An increase in linear density may be a direct consequence of more fiber and binder per unit area, as the fiber mass and binder volume increases.

Table 1: Properties of dry-laid acrylate copolymer nonwoven structures.

Structure	Fiber mass (g)	Binder Vol. (ml)	Ratio g/ml	Density (GS M)	Bursting Strength (MPa)	Absorbency (ml/g)
A	15	15	1	295	0.27	6.92
B	15	10	1.5	274	0.24	7.76
C	15	5	3	241	0.19	8.23
D	10	15	0.7	198	0.17	8.07
E	10	10	1	208	0.15	7.12
F	10	5	2	167	0.13	5.87
G	5	10	0.5	137	0.06	4.57
H	5	5	1	112	0.08	5.05

The role of the binder in the structure serves to link the fibers and thus facilitate the transfer of load between them. This is evident from

Table 1 where at constant fiber mass, a decrease in the applied binder volume results in reduced strengths. Since the fibers used have an average length of about 26mm, a binder is needed to link them up in order to produce a structurally stable structure capable of bearing loads. The load transfer function of the binder can be attributed to its thermosetting properties (Kelly, et al., 2003) where it may provide solid links between the fibers. Apparently, the bursting strength of the fabricated structures compared relatively well with cotton/polyester nonwoven structures produced through thermal-bonding and hydro-entanglement methods (Lewin & Preston, 1993). This is just a relative comparison given the differences in fibers and production methods but it pinpoints the importance of the current fabrication procedure for producing structurally viable nonwoven structures.

The intrinsic absorbency of the structures is relatively low compared to that of bleached cotton fiber of about 24ml/g (Hutten, 2007). Since the fibers used in the current study were not bleached, the presence of hydrophobic cotton wax could have reduced their

water absorbing capacity. It is evident from the

Table 1 that an increase in fiber mass to binder volume ratio leads in many cases to a decrease in water absorption. It is possible that the application of polymeric vinyl-acrylate binder covered the surfaces of cotton fibers further limiting their water absorption capacity.

The macroscopic and microscopic images of structure A are shown in Fig. 1. The macrostructure was relatively uniform and had a smooth texture possibly due to waxy nature of cotton fibers used. However, the microscopic examination revealed random orientation of the fibers and a non-uniform distribution of their area density. Apparently, the fiber bonding in the structure was localized at some nodal points with relatively large lengths of fibers running between the nodes. The exact nature of bonding between the polymeric binder and the untreated cotton fibers is difficult to establish but could be attributed to intermolecular attraction such as polar interactions, hydrogen bonding and nonpolar interactions that may occur between the binder and cotton wax. Formation of chemical bonds such as covalent bonds may not have occurred owing to relatively low curing temperature ($\sim 21^{\circ}\text{C}$) of the binder.

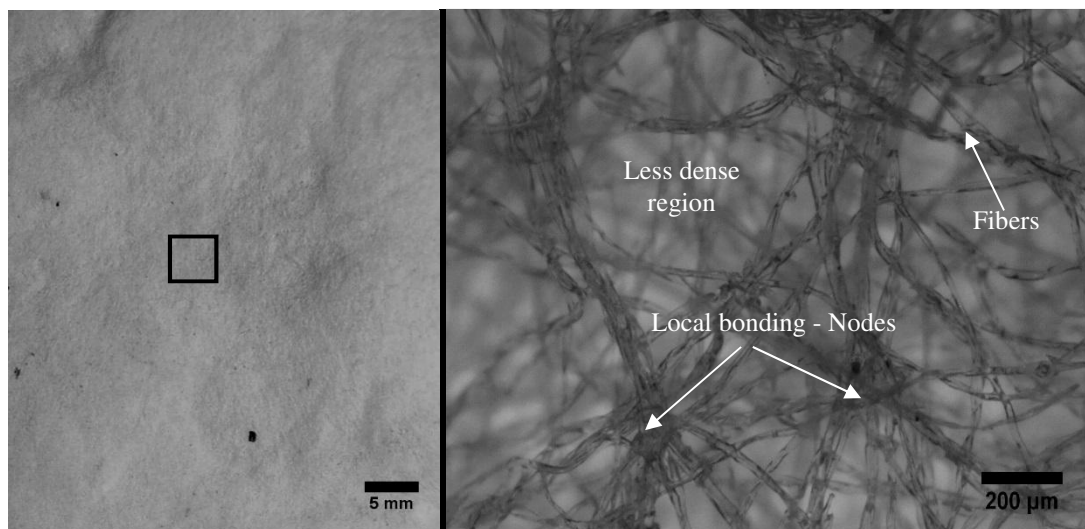


Fig. 1. Nonwoven structure showing: (a) Macrograph at zero strain, and (b) Micrograph of the squared area in (a) indicating local bonding between cotton fibers and less dense regions.

Fig. 2 shows the load-strain curve for structure A which exhibit a ductile failure. The curve has a linear part where deformation is elastic and a non-linear part where permanent deformation occurs. Since the structure is composed of fibers bonded together by a polymeric binder, the elastic deformation may be attributed to extensions in the amorphous part of fiber owing to shear loading of primary and secondary bonds. This elastic strain may also be experienced at the interfaces between binder and fiber and also along the polymer links between the fibers. Plastic deformation in the structure may be attributed to re-arrangement of fiber's long chain molecules as a result of secondary bonds disconnection. This molecular realignment increases the load bearing capacity of the fiber owing to increased intermolecular attraction (Saville, 2002). Consequently, the structure continues to carry additional loads up to

a maximum value after which a reduction in load occurs due to localized deformation (necking) leading to failure. Plastic deformation could also be attributed to relative displacement of fibers during loading since the structure is composed of loosely bound fibers.

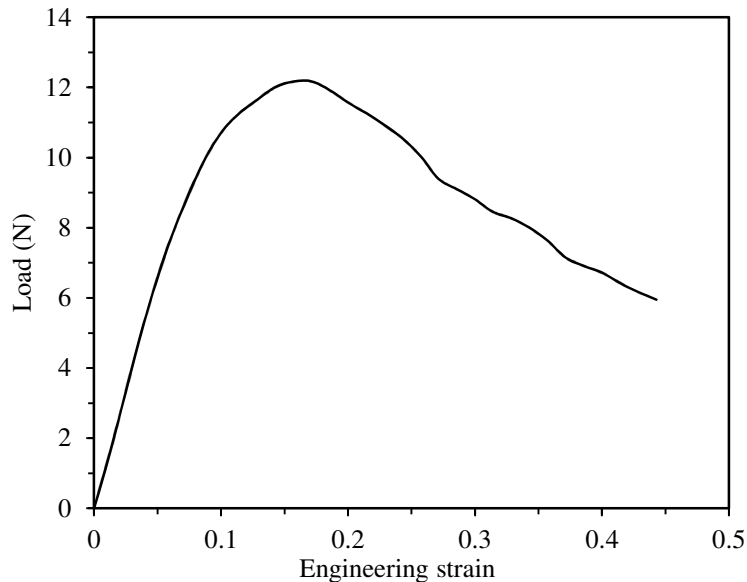


Fig. 2. Load versus engineering strain curve for nonwoven structure having an area density of 295 GSM.

Fig. 3 shows sequential macro-images taken at an engineering strain of 0%, 7%, 14% and 36% and their corresponding vector magnitude maps. Distortion of the structure is evident after 14% engineering strain. Vector magnitude maps were obtained by correlating the image captured at 0% strain with those captured at higher engineering strains. The degree of displacement of surface elements as tracked progressively from their original positions is represented by a rainbow coloring scale. The blue colour indicates the least displacement while the red colour designates the maximum displacement of surface elements as a function of the applied strain. It is evident that the deformation progressed from one end of the structure connected to the moving machine crosshead to the other end. At the point of yielding (~14% strain), the deformation was well distributed throughout the structure while at higher strain (~36%) the deformation remained uniform but some regions, represented by red colour, experienced relatively high strains. These may represent the localized deformation in the weak regions of the structure where failure represented by bond breakdown, fiber rupture or fiber slippage may have originated. The random scatter of these regions may indicate the uniformity of the fiber's bonding in the structure and thus the consistency of its areal mechanical properties.

Apparently, some regions of the structure experienced minimal strain even at the point of failure. This may be attributed to inadequate bonding between the nodal points in the structure (see Fig. 1), which could have lead to poor transmission of the load within these regions. As seen in Fig. 1, this may also represent regions with less fiber coverage and since it

is the fiber movement which is tracked during image correlation, then the regions remains blue. The above assessment portrays a structure with uniform mechanical properties illustrating the success of the stated fabrication method for making structurally stable nonwoven structures.

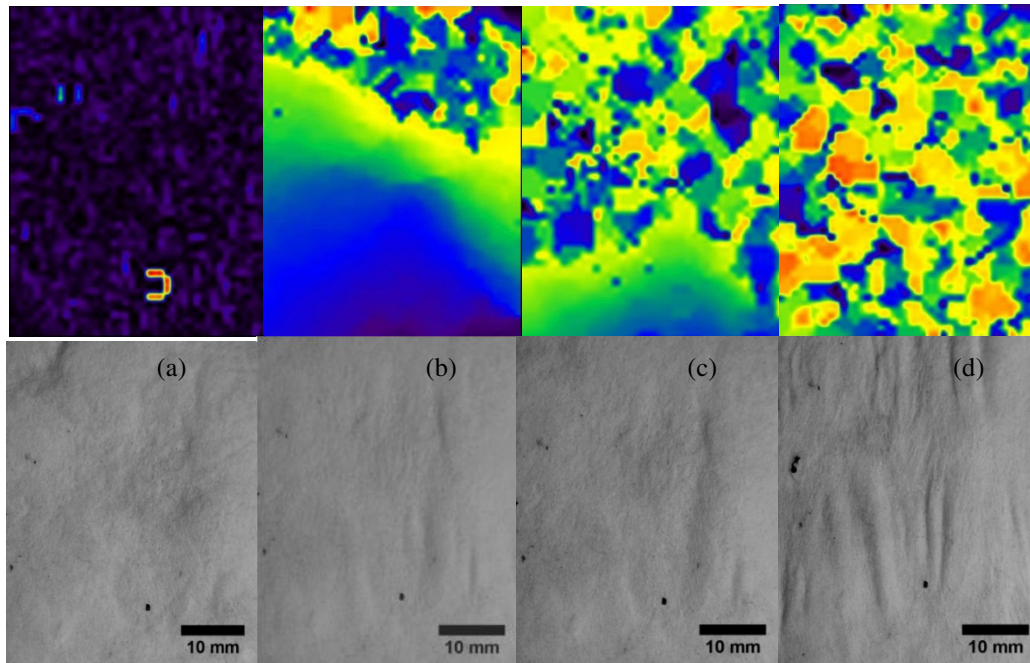


Fig. 3. Macrographs and their corresponding vector magnitude maps for nonwoven structure with: (a) 0%, (b) 7%, (c) 14% and (d) 36% engineering strain. Rainbow colour coding from blue to red represent minimum to maximum strain in the structure.

Fig. 4 shows the variation of average vector magnitude with the engineering strain. A linear correlation is obtained for engineering strain less than 10% and this correspond to the elastic region of the nonwoven structure (see Fig. 2). For strain $> 10\%$, saturation in average vector magnitude occurs which can be attributed to local deformation before failure where elemental displacement on the surface occurs only at limited regions (weak regions represented by red colour) and remains almost the same in other regions. Accordingly, the increase in average vector magnitude per unit strain reduces resulting to saturation. Apparently, the PIV method can be used to assess the state of deformation of nonwoven structure subjected to monotonic loading if its initial condition is digitized in an image. The failure in the structure can easily be predicted from the curves of vector magnitude versus strain.

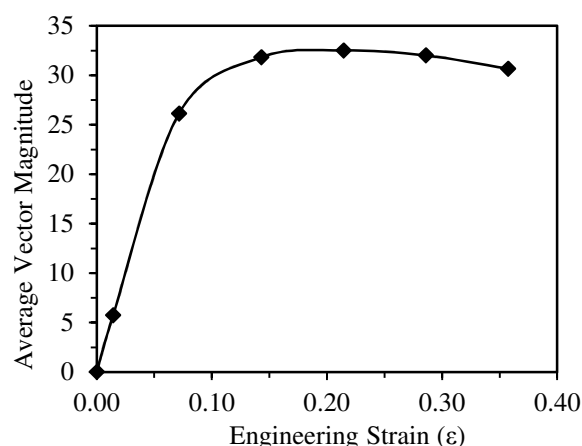


Fig. 4. Variation of average vector magnitude with engineering strain obtained from 295GSM nonwoven structure.

Conclusion

In the current study, a novel method of producing nonwoven structures from dry-laid cotton fibers is presented. The mechanical properties and deformation behavior of the structures is characterized and following conclusions drawn:

- (1) Bonding of dry-laid cotton fibers using atomized acrylate copolymer at room temperature and consolidation pressures of about 2kPa, produces structurally stable nonwoven structure. The structure bursting strength increases with increase in the fiber mass and the applied binder volume while the water absorption reduces with the increase in the volume of the binder applied.
- (2) The nonwoven load-strain curve is characterized by a linear and non-linear behavior corresponding to elastic and inelastic strain, respectively. The structure exhibit a maximum load above which it fails through localized deformation.
- (3) At maximum load the deformation of the nonwoven is relatively uniform but becomes localized as the failure point is approached.
- (4) Image correlation using Particle Image Velocimetry (PIV) method gives both qualitative and quantitative assessment of deformation in the nonwoven structure. The average vector magnitude derived from PIV measurement, correlate well with the engineering strain and can thus be used for strain estimation in similar structures.

Acknowledgement

The authors would like to thank VLIR-OUS for funding this research.

References

- Abramoff, M., Magalhaes, P. J. & Ram, S. J., 2004. Image processing with ImageJ. *Biophotonics international*, 11(7), pp. 36-42.
- Adanur, S., 1995. *Wellington Sears Handbook of Industrial Textiles*. Basel: CRC Press.
- Batra, S. K. & Pourdeyhimi, B., 2012. *Introduction to Nonwovens Technology*. Pennsylvania: DEStech Publications.
- Das, A. & Raghav, R., 2009. Bursting behaviour of spunbonded nonwoven fabrics: effects of various parameter. *Indian Journal of Fibre & Textile Research*, Volume 34, pp. 258-

- 263.
- Desai, A. & Balasubramanian, N., 1994. Critical factors affecting the properties of thermal-bonded nonwovens with special reference to cellulose fibres. *Indian Journal of Fibre & Textile Research*, Volume 19, pp. 209-215.
- Gautier, K. B., Kocher, C. W. & Drean, J. Y., 2007. Anisotropic Mechanical Behavior of Nonwoven Geotextiles Stressed by Uniaxial Tension. *Textile Research Journal*, Volume 77, pp. 20-28.
- Hutten, I. M., 2007. *Handbook of Nonwoven Filter Media*. Delray Beach: Elsevier.
- Kelly, D. P., Melrose, G. J. H. & Solomon, D. H., 2003. Thermosetting vinyl and acrylic copolymers. *Journal of Applied Polymer Science*, 7(6), pp. 1991-2002.
- Lewin, M. & Preston, J., 1993. *Handbook of Fiber Science and Technology Volume 2: High Technology Fibers*. New York: CRC Press.
- Ridruejoa, A., González, C. & LLorca, b. J., 2011. Micromechanisms of deformation and fracture of polypropylene nonwoven fabrics. *International Journal of Solids and Structures*, 48(1), pp. 153-162.
- Russell, S., 2007. *Handbook of Nonwovens*. Cambridge: Woodhead Publishing.
- Saville, B., 2002. *Physical testing of textiles*. Cambridge: Woodhead Publishing.
- Wang, R., Xu, B. & Li, C., 2014. Accurate fiber orientation measurements in nonwovens using a multi-focus image fusion technique. *Textile Research Journal* , 84(2), pp. 115-124.
- Westerweel, J., 1993. *Digital Particle Image Velocimetry: Theory and Application*. Delft: Delft University Press.
- Westerweel, j., 1997. Fundamental of digital particle image velocimetry. *Measurement Science and Technology*, Volume 8, pp. 1379-1392.
- Westerweel, J., 2000. Theoretical analysis of the measurement precision in particle image velocimetry. *Experiments in Fluids*, Volume 29, pp. 3-12.
- Willert, C. E., 1996. The fully digital evaluation of photographic PIV recordings. *Applied Scientific Research*, Volume 56, pp. 79-102.
- Willert, C. E. & Gharib, M., 1991. Digital Particle Image Velocimetry. *Experiments in Fluids*, Volume 10, pp. 181-193.